0013-7227/07/$15.00/0
Printed in U.S.A.

Endocrinology 148(10):4548–4556

doi: 10.1210/en.2006-1371

Chronic Blockade of Nitric Oxide Synthesis Reduces Adiposity and Improves Insulin Resistance in High Fat-Induced Obese Mice

Kyoichiro Tsuchiya, Haruna Sakai, Noriko Suzuki, Fumiko Iwashima, Takanobu Yoshimoto, Masayoshi Shichiri, and Yukio Hirata

Department of Clinical and Molecular Endocrinology, Tokyo Medical and Dental University Graduate School, Tokyo 113-8519, Japan

Genetic deletion of inducible nitric oxide synthase (NOS) in mice has been shown to improve high-fat diet (HFD)-induced insulin resistance. However, a pathophysiological role of endogenous nitric oxide (NO) in obesity-related insulin resistance remains controversial. To address this issue, we examined the metabolic phenotypes in HFD-induced obese mice with chronic blockade of NO synthesis by a NOS inhibitor, *N*(G)-nitro-L-arginine methyl ester (L-NAME). Six-week-old male C57BL/6j mice were provided free access to either a standard diet (SD) or a HFD and tap water with or without L-NAME (100 mg/kg·d) for 12 wk. L-NAME treatment significantly attenuated body weight gain of mice fed either SD or HFD without affecting calorie intake. L-NAME treatment in HFD-fed mice improved glucose tolerance and insulin sensitivity. HFD feeding induced inducible NOS mRNA expression, but not the other two NOS isoforms, in white adipose tissue (WAT) and skeletal muscle. L-NAME treatment up-regulated uncoupling protein-1 in brown adipose tissue of HFD-fed mice but down-regulated monocyte chemoattractant protein-1 and CD68 mRNAs levels in WAT. HFD feeding up-regulated leptin mRNA levels but conversely down-regulated adiponectin mRNA levels in WAT, but these effects were unaffected by L-NAME treatment. Moreover, L-NAME treatment also increased peroxisome proliferator-uncoupling protein-3 mRNA levels in skeletal muscles of HFD-fed mice. Increased urinary excretion of norepinephrine after HFD feeding was augmented in L-NAME-treated mice. Insulin-stimulated tyrosine phosphorylation of insulin receptor substrate-1 and serine phosphorylation of Akt/Akt2 in soleus muscle was markedly impaired in HFD-fed mice but reversed by L-NAME treatment. In conclusion, chronic NOS blockade by L-NAME in mice ameliorates HFD-induced adiposity and glucose intolerance, accompanied by reduced adipose inflammation and improved insulin signaling in skeletal muscle, suggesting that endogenous NO plays a modulatory role in the development of obesity-related insulin resistance. (*Endocrinology* 148: 4548–4556, 2007)

NITRIC OXIDE (NO) is a unique gas molecule that plays pivotal messenger roles in a wide variety of physiological functions, including neuronal transmission, vascular relaxation, immune modulation, and cytotoxicity (1). Recent accumulating lines of evidence have also suggested the role for NO in the control of lipid and glucose metabolism. It has been reported that blockade of endogenous NO by a NO synthase (NOS) inhibitor, *N*(G)-monomethyl-L-arginine, increases lipolysis (2), whereas NO donors reduce glycerol release in human adipocytes (3) and inhibit insulin-stimulated glucose transport in rat myocytes *in vitro* (4). On the contrary, stimulatory effect of NO on glucose uptake in rat skeletal muscle has been reported (5).

There are at least three isoforms of NOS: endothelial (eNOS), neuronal (nNOS), and inducible (iNOS) types. iNOS synthesized *de novo* in response to a number of inflammatory stimuli, such as proinflammatory cytokines and bacterial endotoxins, produce large amounts of NO over prolonged periods of time (6). In mice, eNOS and nNOS, both constitutively expressed in white adipose tissue (WAT) and skeletal muscle, did not change after high-fat feeding (7). On the other hand, iNOS expression barely detectable in WAT and skeletal muscle in mice markedly increased after high-fat feeding (7). It is therefore assumed that both eNOS and nNOS in WAT and skeletal muscle locally produce small amounts of NO under normal conditions, whereas increased expression of iNOS in obese state could produce large quantities of NO, which may partly contribute to the development of obesity-related glucose intolerance.

Metabolic phenotypes obtained from the animal models lacking respective NOS genes have been inconsistent. Mice disrupted of eNOS and/or nNOS gene exhibit the metabolic syndrome, including insulin resistance, hypertension, and dyslipidemia (8), whereas induction of iNOS by endotoxin is associated with impaired insulin-stimulated muscle glucose uptake (4). Conversely, iNOS null mice, although protected from obesity-related insulin resistance, showed increased adiposity (7). Furthermore, treatment with an iNOS-selective inhibitor, L-N(6)-(1-iminoethyl)lysine, reversed fasting hyperglycemia with concomitant amelioration of hyperinsulinemia and improved insulin sensitivity in *ob/ob* mice (9).

First Published Online June 21, 2007

Abbreviations: AP, Activator protein; BAT, brown adipose tissue; eNOS, endothelial NOS; HFD, high-fat diet; iNOS, inducible NOS; IR, insulin receptor; IRS, insulin receptor substrate; L-NAME, *N*(G)-nitro-L-arginine methyl ester; MCP, monocyte chemoattractant protein; nNOS, neuronal NOS; NO, nitric oxide; NOS, nitric oxide synthase; NOx, nitrite/nitrate; PPAR, peroxisome proliferator-activated receptor; SD, standard diet; UCP, uncoupling protein; WAT, white adipose tissue.

***Endocrinology* is published monthly by The Endocrine Society (http://www.endo-society.org), the foremost professional society serving the endocrine community.**

There have been several reports showing pharmacological effect of chronic blockade, by *N*(G)-nitro-L-arginine methyl ester (L-NAME), a NOS inhibitor, in obese rodents (10–13). Although NO is shown to be involved in the regulation of body weight and insulin resistance, its chronic effect on high-fat diet (HFD)-induced obesity and insulin resistance remains unknown.

Obesity is associated with increased macrophage infiltration in adipose tissue (14). The activated macrophage, a major source of proinflammatory factors, could play an important role in the development of insulin resistance (15). Monocyte chemoattractant protein (MCP)-1, a potent chemotactic factor for monocytes (16), has been shown to contribute to macrophage infiltration into adipose tissue (15). Several key metabolic factors, such as adipocyte-derived hormones (leptin, adiponectin), energy uncoupling regulators, uncoupling proteins (UCPs) (17), and fatty acid catabolism enhancer, peroxisome proliferator-activated receptor (PPAR)-δ (18), have been shown to affect the development of diet-induced obesity and glucose intolerance. On the other hand, NO blockade with NOS inhibitors induce vascular inflammation with enhanced expression of several proinflammatory genes, including MCP-1 (19), in cardiovascular tissue. However, it remains unknown whether NO affects genes expression of the above-mentioned inflammation-related and metabolic factors in obesity.

These observations led us to examine whether NO contributes to diet-induced obesity, adiposity, glucose metabolism, and inflammation- and metabolic-related genes expression in mice by blockade of NO synthesis with a NOS inhibitor, L-NAME.

Materials and Methods

Animal experiments

Six-week-old male C57BL/6j mice (Oriental Yeast, Tokyo, Japan) were maintained in temperature- and humidity-controlled rooms illuminated from 0800 to 2000 h. They were fed *ad libitum* with either a standard diet (SD; 3.6 kcal/g, 5.4% energy as fat) or a HFD (6.4 kcal/g, 82% energy as fat) and were allowed free access to tap water with or without L-NAME (100 mg/kg·d; Sigma-Aldrich, Co., St. Louis, MO) for 12 wk. Body weights were measured every 2 wk, and food intake as calories was calculated from consumed food weight. At the end of 10 and 11 wk, they received glucose and insulin tolerance tests, respectively. At the end of 12 wk, they were placed in metabolic cages for 24-h urine collection. Blood samples were obtained from femoral vein, and after measurement of systolic blood pressure by the indirect tail-cuff method (BP-98A; Softron, Tokyo, Japan), they were killed under pentobarbital anesthesia for the analyses of organs and tissues. No mice died during the entire 12-wk period after L-NAME treatment. All experiments were conducted in accordance with the Tokyo Medical and Dental University Guideline for the Care and Use of Experimental Animals.

Glucose and insulin tolerance tests

Mice fed on either a SD or HFD for 10 wk were fasted for 6 h and injected ip with glucose (1 g/kg body weight). A week later, regular insulin (0.75 IU/kg body weight; Humulin R-Insulin; Eli Lilly & Co., Indianapolis, IN) was injected ip after a 2-h fast. Blood was withdrawn from the tail vein before and at indicated times after injections for measurement of plasma glucose concentrations.

Measurement of blood and urinary parameters

Blood glucose was measured by the blood glucose test meter (Glu test Ace; Sanwa-Kagaku Co., Nagoya, Japan), serum triglyceride by a Triglyceride-E reagent kits (Wako Pure Chemical Industries Ltd., Osaka, Japan), serum insulin by an ELISA kit (Morinaga, Co., Tokyo, Japan), urinary nitrite/nitrate (NOx), and catecholamine by the Griess method (20) and reverse-phase HPLC (21), respectively.

Histological analysis

Tissue weights of the epididymal, sc, and mesenteric WAT, and liver excised from mice fed on a SD or HFD for 12 wk were measured. Portions of epididymal adipose tissue and liver were fixed with 10% formalin and embedded in paraffin. Sections were stained with hematoxylin-eosin. The adipocyte areas were measured using ImageJ software (National Institute of Mental Health, Bethesda, MD).

Measurement of hepatic triglyceride content

Hepatic tissue (200 mg) was homogenized at 4 C in 4 ml of a mixture of $CHCl_3$-MeOH (2:1; vol/vol) using a Polytron homogenizer. After adding 1 ml of distilled water, the resulting suspension was vigorously mixed and centrifuged at 2000 × *g* for 10 min. The chloroform-methanol layer was removed and evaporated. The lipid residue was resuspended in 1% Triton X-100 in absolute EtOH, and triglyceride concentrations were determined.

Quantitative real-time RT-PCR

Total RNAs from mouse epididymal WAT, interscapular brown adipose tissue (BAT), liver, and soleus muscle were extracted using Trizol reagent (Invitrogen, Co., Carlsbad, CA), and equal amounts of total RNA were reverse transcribed with the Omniscript reverse transcription kit (QIAGEN, Inc., Valencia, CA), using random hexamers, according to the manufacturers' instruction. The mRNA levels of mouse β-actin, iNOS, eNOS, nNOS, CD68, adiponectin, leptin, PPAR-δ, UCP-1, and UCP-3 were quantified using a LightCycler fluorescent SYBR green technology (Roche Molecular Biochemicals, Mannheim, Germany) as described previously (22). Mouse MCP-1 mRNA levels were quantified with real-time RT-PCR based on Taqman chemistry using a LightCycler as described previously (22). PCR primers and TaqMan hybridization probes and sizes of each PCR product are listed in Table 1. The mRNA levels of the target sequences were normalized by those of β-actin used as an endogenous internal control; the relative levels of each mRNA to that of β-actin were calculated.

Immunoprecipitation and immunoblotting

Six-hour fasted mice were injected with saline or insulin (1.3 IU/kg) via the portal vein, and after 3 min soleus muscle was excised and homogenized with lysis buffer containing 20 mM Tris (pH 7.4), 10 mM sodium pyrophosphate, 100 mM NaF, 5 mM EDTA, 5 mM sodium orthovanadate, 0.1 mg/ml aprotinin, 2 mM phenylmethylsulfonyl fluoride, and 1% Nonidet P-40. After centrifugation at 14,000 × *g* for 10 min, the supernatant was subjected for subsequent analysis.

Tyrosine phosphorylation of insulin receptor (IR)-β and insulin receptor substrate (IRS)-1, and serine phosphorylation of Akt2 were analyzed by immunoprecipitation followed by immunoblotting. For immunoprecipitation, anti-IR-β, anti-IRS-1 antibody (Upstate Biotechnology, Lake Placid, NY), or anti-Akt2 antibody (Cell Signaling Technology Inc., Danvers, MA) was added to the lysate (0.7–1.5 mg). Volume was adjusted to 700 μl with lysis buffer and then mixed for 12 h at 4 C. Protein G agarose beads (Zymed Laboratories, San Francisco, CA) were added (15 μl bed volume) to the lysate, and the mixture was inverted at 4 C for an additional 2 h. The beads were washed three times with wash buffer containing 150 mM NaCl, 50 mM HEPES (pH 7.4), 5 mM EDTA, and 1% Nonidet P-40 solubilized in Laemmli sample buffer, and then supernatant was used for Western blot analysis. Serine phosphorylation of Akt was directly analyzed by immunoblotting.

Immunoprecipitates or equal amounts of skeletal muscle and adipose tissue lysate were subjected to SDS-PAGE, and immunoblotted with antiphosphotyrosine (4G10; Upstate Biotechnology), antiphosphoserine-307-IRS-1 (Cell Signaling Technology), antiphosphoserine-473-Akt, and antiphosphoserine-Akt2 (Cell Signaling Technology), respectively. Immunoblottings of adipose tissue were performed using anti-MCP-1 antibody (R&D Systems, Minneapolis, MN), anti-CD68 antibody (AbD Serotec, Raleigh, NC), and anti-UCP-1 antibody (Sigma, St. Louis, MO); the band intensities were quantified using ImageJ software (National Institute of Mental Health).

TABLE 1. Sequences of the PCR primers used for real-time RT-PCR in this study

PCR product		Primer sequence (5′–3′)	PCR product size
β-Actin	F	CCCTAAGGCCAACCGTGAAA	101
	R	AGGCATACAGGGACAGCACA	
iNOS	F	CAGCTGGGCTGTACAAACCTT	94
	R	CATTGGAAGTGAAGCGTTTCG	
eNOS	F	GCACTACGGTGTCTGCTCCA	115
	R	TGCAGGGCAAGTTAGGATCA	
nNOS	F	GGCCATCGTGTCCTACCATA	96
	R	GACGACATCGTCAGCCTGTA	
CD68	F	CTTCCCACAGGCAGCACAG	235
	R	AATGATGAGAGGCAGCAAGAGG	
Adiponectin	F	ATGGCAGAGATGGCACTCCT	105
	R	ATGGCAGAGATGGCACTCC	
Leptin	F	TCACACACGCAGTCGGTATC	129
	R	GCTGGTGAGGACCTGTTGAT	
UCP-1	F	TACCCAAGCGTACCAAGCTG	100
	R	AGGACCCGAGTCGCAGAAAA	
PPAR-δ	F	AGTGACCTGGCGCTCTTCAT	111
	R	TTCTAGAGCCCGCAGAATGG	
UCP-3	F	GACCCACGGCCTTCTACAAA	125
	R	TTCCCGCAGTACCTGGACTT	
MCP-1	F	AGGTCCCTGTCATGCTTCTG	92
	R	GAGTGGGGCGTTAACTGCAT	
	T	CTGTTCACAGTTGCCGGCTGGAGCATCCAC	

F, Forward primer; R, reverse primer; T, TaqMan probe.

Statistical analysis

Data were expressed as mean ± SE. Differences between groups were examined for statistical significance using unpaired *t* test or ANOVA with Dunn's *post hoc* test, if appropriate. $P < 0.05$ were considered statistically significant.

Results

Changes of blood pressure and body and tissue weights

We examined the effect of L-NAME treatment on the changes of blood pressure and weights of whole body, various adipose tissues, and liver in SD- and HFD-fed mice. L-NAME treatment significantly ($P < 0.01$) increased systolic blood pressure and decreased heart rate (Table 2). Body weight gains of SD- and HFD-fed mice were significantly ($P < 0.05$) reduced in L-NAME-treated groups more than those in the corresponding vehicle-treated groups on the same diet (Fig. 1A). Both SD- and HFD-fed mice showed significantly ($P < 0.05$) reduced cumulative caloric intake during the initial 8- and 4-wk L-NAME treatment period, respectively, after which there was no such difference to the end of experiments (Fig. 1B). Food intake corrected for body weight increased in L-NAME-treated mice (Table 2). Daily spillage of food determined repeatedly in a separate set of experiments, was statistically not different among four groups: SD fed, vehicle treated (212 ± 57 mg/animal · d); SD fed, L-NAME treated

TABLE 2. Several parameters of mice fed a SD and HFD after treatment with or without NOS inhibitor

	SD		HFD	
L-NAME treatment	(−)	(+)	(−)	(+)
Systolic blood pressure (mm Hg)	115 ± 3	144 ± 3[a]	112 ± 1	144 ± 2[b]
Heart rate (beat/min)	686 ± 10	599 ± 16[a]	714 ± 5	670 ± 9[b]
Caloric intake (kcal per 30 g/d)[c]	10.3 ± 0.2	10.9 ± 0.2[d]	11.1 ± 0.2[a]	12.5 ± 0.7[b]
Tissue weight (g)				
Adipose tissue				
Epididymal	0.42 ± 0.03	0.33 ± 0.03[d]	2.84 ± 0.25[a]	1.99 ± 0.31[b]
Mesenteric	0.17 ± 0.01	0.16 ± 0.01	0.65 ± 0.05[a]	0.43 ± 0.05[b]
Subcutaneous	0.25 ± 0.02	0.17 ± 0.02[d]	1.20 ± 0.07[a]	0.58 ± 0.10[b]
Liver	0.94 ± 0.06	0.92 ± 0.01	1.43 ± 0.06[d]	1.12 ± 0.03[b]
Blood glucose (mg/dl)	136 ± 3	128 ± 6	190 ± 8[a]	138 ± 19[b]
Serum insulin (ng/ml)	0.8 ± 0.2	1.1 ± 0.2	1.6 ± 0.3[d]	1.1 ± 0.2[b]
Serum triglyceride (mg/dl)	91 ± 14	97 ± 7	149 ± 20[d]	118 ± 26[d]
Urinary excretion (ng/d)				
Epinephrine	34 ± 3	39 ± 5	56 ± 4[d]	59 ± 8[d]
Norepinephrine	343 ± 22	449 ± 44[d]	466 ± 40[d]	614 ± 34[b]

−, Treatment without NOS inhibitor; +, treatment with NOS inhibitor.

[a] $P < 0.01$ as compared with vehicle-treated mice on SD.

[b] $P < 0.05$ as compared with vehicle-treated mice on HFD.

[c] Adjusted for body weight: daily caloric intake divided by the average body weight and multiplied by 30. All data were obtained at 12 wk after treatment with or without L-NAME.

[d] $P < 0.05$ as compared with vehicle-treated mice on SD.

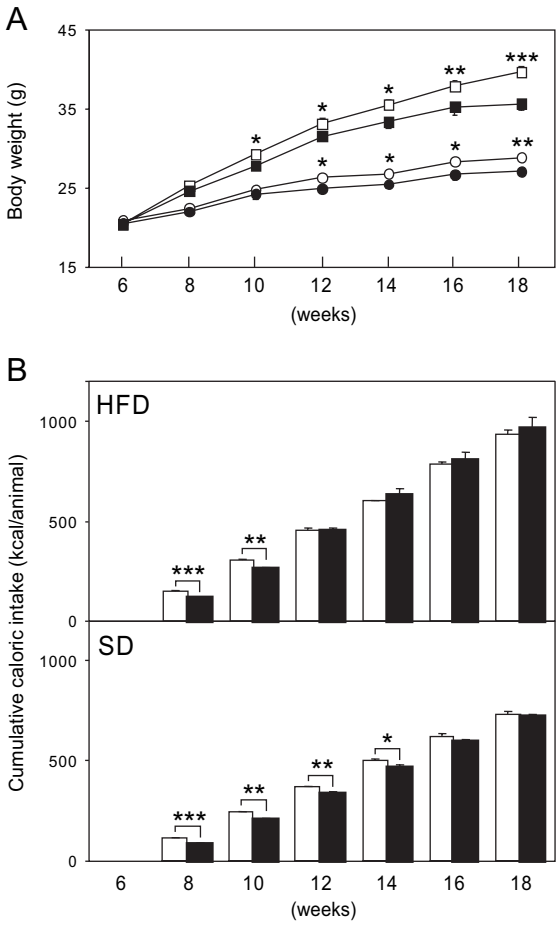

FIG. 1. Changes of body weight and cumulative caloric intake of mice fed SD and HFD with or without NOS inhibitor. A, Body weights of C57BL/6j mice fed a SD (*circle*) or HFD (*square*) treated with (*closed circle*) or without (*open circle*) L-NAME were measured biweekly during 6–18 wk of age. B, Cumulative caloric intake of mice fed a SD (*upper panel*) or HFD (*lower panel*) treated with (*black column*) or without (*white column*) L-NAME was measured. Each *symbol* and *column* represents means ± SE from six independent animals. *, $P < 0.05$, **, $P < 0.01$, and ***, $P < 0.001$ between the indicated groups.

(228 ± 70 mg/animal · d); HFD fed, vehicle treated (321 ± 133 g/animal · d); and HFD fed, L-NAME treated (283 ± 117 g/animal · d). Rectum temperature at 8 wk after treatment with or without L-NAME was statistically not different among four groups; SD fed, vehicle treated (37.6 ± 0.3 C); SD fed, L-NAME treated (37.9 ± 0.5 C); HFD fed, vehicle treated (37.7 ± 0.5 C); and HFD fed, L-NAME treated (37.8 ± 0.4 C). Locomotor activity using walking track analysis of footprints did not show any statistical differences between vehicle- and L-NAME-treated fed on SD or HFD (data not shown).

The weights of the epididymal, sc, and mesenteric WAT and the liver were significantly ($P < 0.05$) greater in vehicle-treated HFD-fed mice than in SD-fed mice. L-NAME treatment significantly ($P < 0.05$) reduced their weights in HFD-fed mice (Table 2). These data show that inhibition of body weight gain by L-NAME treatment is accompanied by reduced adiposity.

Histological examination of epididymal WAT and hepatic tissue (Fig. 2A) and hepatic lipid content revealed that HFD-fed mice had markedly increased adipocyte size (Fig. 2B) and hepatic lipid accumulation more than did SD-fed mice (Fig. 2C). L-NAME markedly suppressed epididymal adiposity and hepatic lipid accumulation in HFD-fed mice, whereas L-NAME treatment did not appreciably affect adipocyte size or hepatic lipid accumulation in SD-fed mice (Fig. 2).

Changes of glucose tolerance and insulin sensitivity

Fasting blood glucose and serum insulin concentrations were significantly ($P < 0.05$) higher in vehicle-treated HFD-fed mice than those in SD-fed mice (Table 2), both of which significantly ($P < 0.05$) decreased in L-NAME-treated groups. Glucose tolerance tests showed that HFD-fed mice showed impaired glucose tolerance as compared with SD-fed mice (Fig. 3A). However, glucose intolerance in HFD-fed mice was significantly ($P < 0.05$) improved by L-NAME treatment; blood glucose levels at 30 and 60 min after the glucose bolus were significantly ($P < 0.05$) lower in HFD-fed mice treated with L-NAME than those without L-NAME. Serum insulin levels at baseline and 30 and 60 min after glucose injection were significantly not different between vehicle- and L-NAME-treated mice fed on SD or HFD (supplemental Fig. 1, published as supplemental data on The Endocrine Society's Journals Online web site at http://endo.endojournals.org). Whole-body insulin sensitivity for glucose disposal as assessed by insulin tolerance test showed that hypoglycemic effect was attenuated in HFD-fed mice as compared with that in SD-fed control mice, whose effect was reversed by L-NAME treatment (Fig. 3B). These observations suggest that L-NAME treatment improves HFD-induced glucose intolerance and insulin resistance.

Changes of urinary excretions of catecholamine and NOx

To determine sympathetic nerve activity in L-NAME treatment, we measured 24-h urinary catecholamine excretion. Urinary excretions of epinephrine and norepinephrine were significantly ($P < 0.05$) increased in HFD-fed mice more than those in SD-fed mice, whereas L-NAME treatment significantly ($P < 0.05$) increased urinary excretion of norepinephrine, but not epinephrine, in mice on either SD or HFD (Table 2). These observations suggest that increased sympathetic nerve activity by L-NAME treatment is partly involved in attenuating weight gain induced by L-NAME treatment. Inhibition of NO synthesis by L-NAME treatment was confirmed by reduction of 24 h urinary NOx excretion of SD- and HFD-fed groups by 53–63%, compared with control group (data not shown).

NOS isoform gene expression in adipose tissue and skeletal muscle

The effect of HFD-induced obesity on gene expression of three NOS isoforms in epididymal WAT, interscapular BAT, and skeletal muscle were determined (Fig. 4). In epididymal WAT, HFD feeding significantly ($P < 0.05$) up-regulated iNOS mRNA levels but did not affect eNOS mRNA expression, whereas basal nNOS mRNA level was undetectable (Fig. 4A). In BAT, however, iNOS or eNOS mRNA expres-

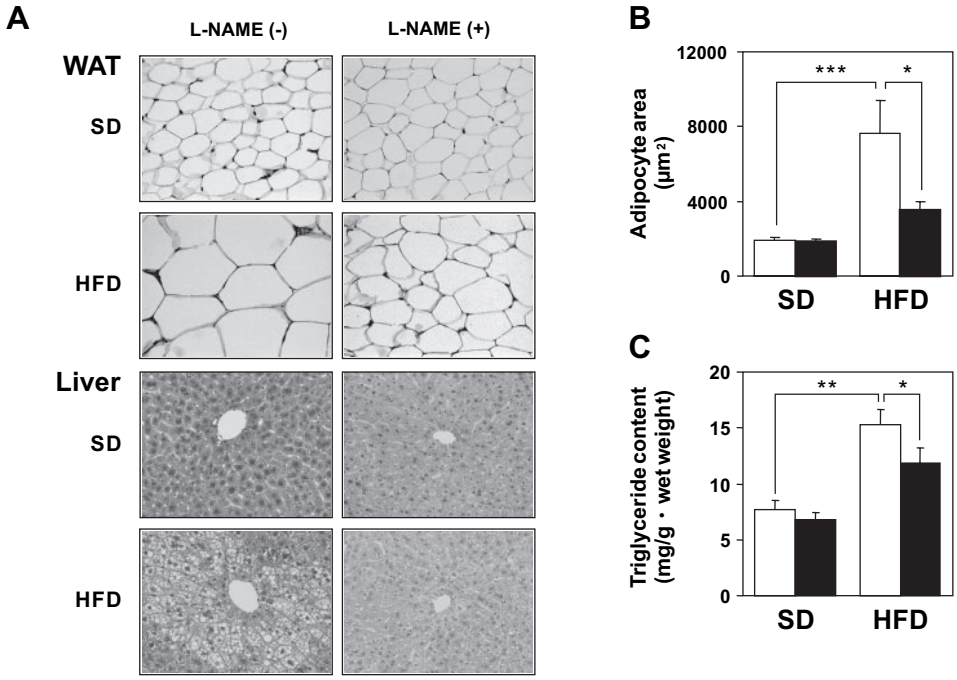

FIG. 2. Histological changes of adipose and hepatic tissue and hepatic triglyceride contents. A, Hematoxylin-eosin staining of epididymal WAT and liver from SD- or HFD-fed mice treated with or without L-NAME (open magnification, ×200). B, Adipocyte areas in epididymal WAT from SD- or HFD-fed mice treated with (*black column*) or without (*white column*) L-NAME are shown; adipocyte cell sizes in four independent scanned microscopic sections from each of five independent animal were measured. C, Hepatic triglyceride content of SD- or HFD-fed mice treated with (*black column*) or without (*white column*) L-NAME. Each *column* is the mean of six independent animals. *, $P < 0.05$, **, $P < 0.01$, and ***, $P < 0.001$ between the indicated groups.

sion did not change after HFD feeding, and basal nNOS mRNA level was undetectable (Fig. 4B). In skeletal muscle, HFD feeding also significantly ($P < 0.01$) induced mRNA expression for iNOS but not for eNOS or nNOS (Fig. 4C). These data suggest that NO production induced by HFD feeding in WAT and skeletal muscle is mainly mediated via iNOS induction.

Inflammation- and metabolism-related gene and protein expression in adipose tissue and skeletal muscle

To gain further insight into the underlying molecular mechanisms of attenuated adiposity and improved glucose intolerance in L-NAME-treated mice, we examined the changes of expression of a number of important genes and proteins involved in inflammation (MCP-1, CD68), glucose and lipid metabolism (adiponectin, PPAR-δ, UCP-3), and thermogenesis (leptin, UCP-1 and -3) in adipose tissue and skeletal muscle (Fig. 5). In epididymal WAT (Fig. 5A), both MCP-1 and CD68 mRNA and protein levels were significantly increased by HFD, whose effect was blocked by L-NAME treatment. HFD significantly ($P < 0.01$) down-regulated adiponectin mRNA levels but conversely up-regulated leptin mRNA levels; these effects were either unaffected or decreased by L-NAME treatment. In skeletal muscle (Fig. 5B), L-NAME increased both PPAR-δ and UCP-3 mRNA levels in HFD-fed mice but not SD-fed mice. In contrast, L-NAME significantly ($P < 0.05$) decreased iNOS mRNA levels in both SD- and HFD-fed mice (supplemental Fig. 2). In interscapular BAT (Fig. 5C), L-NAME significantly ($P < 0.05$) increased UCP-1 mRNA levels in both SD- and HFD-fed mice and its protein levels in HFD-fed mice. These data suggest that attenuated adiposity and improved glucose intolerance in L-NAME-treated mice are functionally related to decreased adipose inflammation, enhanced lipid disposal, and increased thermogenesis in peripheral tissues.

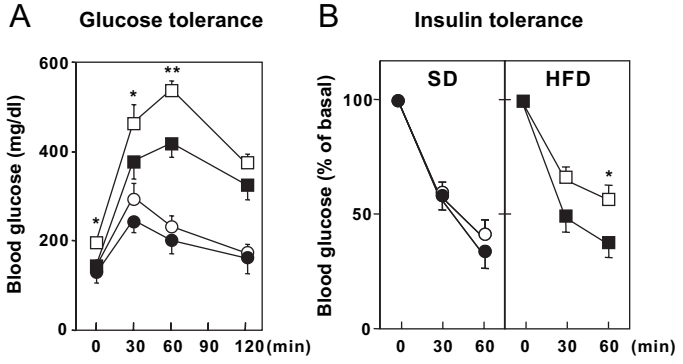

FIG. 3. Changes of glucose tolerance and insulin sensitivity. Blood glucose levels were measured before and after glucose (A) and insulin tolerance (B) tests in SD (*circle*)- and HFD (*square*)-fed mice treated with (*closed*) or without (*open*) L-NAME. Each *symbol* represents means ± SE from six to nine independent animals. *, $P < 0.05$ and **, $P < 0.01$ *vs.* HFD-fed mice treated with L-NAME.

Insulin signaling in skeletal muscle

Finally, to investigate the effect of chronic NO inhibition on insulin signaling in skeletal muscle, we examined insulin-stimulated tyrosine phosphorylation of IR-β and IRS-1 and serine phosphorylation of Akt/Akt2 in soleus muscle from L-NAME-treated mice (Fig. 6). Insulin-stimulated tyrosine phosphorylation of IR-β was unaffected in HFD- and SD-fed mice treated with or without L-NAME. By contrast, insulin-stimulated phosphorylation of IRS-1 significantly ($P < 0.05$) decreased in HFD-fed mice, compared with SD-fed mice, whose effect was abrogated by L-NAME treatment (Fig. 6A). HFD significantly ($P < 0.05$) increased serine-307 phosphorylation of IRS-1, but there were no significant differences between vehicle- and L-NAME-treated mice fed on SD or HFD (supplemental Fig. 3). Furthermore, insulin-stimulated serine phosphorylation of both Akt and Akt2 was markedly

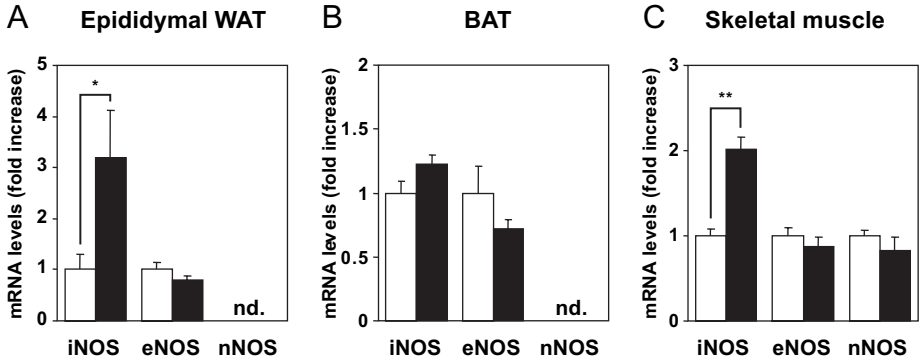

FIG. 4. Changes of NOS isoform gene expression in adipose tissue and skeletal muscle. Steady-state mRNA levels for three NOS isoforms (iNOS, eNOS, nNOS) determined by real-time quantitative RT-PCR in epididymal WAT (A), interscapular BAT (B), and skeletal muscle (C) of SD-fed (*white column*) and HFD-fed (*black column*) mice. Each *column* is the mean of six independent animals expressed as fold increase over control SD-fed mice. *, $P < 0.05$ and **, $P < 0.01$ between the indicated groups. nd, Not detected.

impaired by HFD feeding, whose effect was ameliorated by L-NAME treatment (Fig. 6B). These data suggest that HFD-induced glucose intolerance and impaired insulin signaling, including phosphorylation of IRS-1 and Akt/Akt2, are partly mediated via NO-dependent mechanism.

Discussion

The present study clearly demonstrates that HFD-induced obese mice treated with a chronic NOS inhibitor exhibited marked attenuation of weight gain and adiposity, accompanied by decreased adipose inflammation and enhanced insulin signaling in skeletal muscle. Such improved insulin resistance of the L-NAME-treated mice fed on HFD as demonstrated in this study appears to be similar to those of iNOS-null mice, except that iNOS-null mice consumed more food than their wild-type counterparts and showed increased adiposity after HFD feeding (7). This is in contrast to the decreased adiposity without any change in total calorie intake in the L-NAME-treated mice fed on HFD in our study. Although the precise mechanism(s) by which iNOS-null mice is prone to be hyperphagic remains unknown, it is rational to speculate that iNOS gene deletion could affect eating behavior.

There have been several studies showing conflicting results regarding the effects of L-NAME treatment on food intake in rodents (10–13, 23, 24). It has been shown that short-term NO inhibition by L-NAME reduced food intake, possibly due to a central effect, thereby leading to weight loss and decreased glucose levels (11, 12). On the other hands, obese and Wistar rats treated with L-NAME for longer periods (6 and 12 wk, respectively) showed unaltered cumulative caloric intake (23, 24). Our study showed reduced caloric intake during the initial 8- and 4-wk L-NAME treatment in SD- and HFD-fed mice, but the differences disappeared by the end of 12 wk treatment. Therefore, decreased caloric intake during the initial period of L-NAME treatment could contribute to the attenuated weight gain, but decreased adiposity during the long-term L-NAME treatment did not result from altered caloric intake.

Body weight gain was lower, but caloric intake corrected by body weight in L-NAME-treated HFD-fed mice was higher than that in the corresponding vehicle-treated mice, suggesting increased energy expenditure. The difference in weight gain between the two groups calculated from the final body weights was 57 mg/d, representing only a small portion of the daily caloric intake (0.40 kcal/d), assuming that this is all fat, but this amount should lead to a significant difference after long-term L-NAME treatment. Daily spillage of food was almost the same between SD- and HFD-fed mice. Furthermore, sample size (six animals in SD- and HFD-fed groups) has 80% power to detect such small differences of mean values as low as 1.10 and 1.97 kcal/d per animal, respectively (both at a significance level of 0.05). Assuming that these caloric differences accumulated for 12 wk, they correspond to 13 and 24 mg/animal in SD- and HFD-fed mice, respectively, when converted to fat. Our experimental design is considered to be sufficient enough to detect the differences in food intake to account for the differences in adiposity. Thus, it is reasonable to conclude that reduced adiposity in L-NAME-treated HFD-fed mice observed in the present study is most likely due to increased energy expenditure rather than reduced caloric intake.

The present results with increased urinary norepinephrine excretion after L-NAME treatment is consistent with the enhanced sympathetic nerve activity resulting from chronic blockade of endogenous NO production, based on the previous observations that chronic NO blockade increased circulating catecholamines concentrations, their turnover and reuptake in rats (25, 26), and enhanced sympathetic nerve activity at both pre- and postjunctional sites in dogs (27). Because catecholamines activate lipolysis via β-adrenoreceptors (28), the enhanced sympathetic nerve activity could contribute to decreased adiposity in L-NAME-treated mice fed on a HFD.

The present study shows that UCP-1, a member of mitochondrial transporter superfamily that increases energy expenditure by proton flux across the inner mitochondrial membrane (29), is up-regulated in interscapular BAT after L-NAME treatment. Because β-adrenergic stimulation of BAT has been shown to induce UCP-1 expression (30), the decreased adiposity after L-NAME treatment is likely due in part to increasing energy expenditure via induction of UCP-1 resulting from the enhanced sympathetic nerve activity.

The present study further shows a marked down-regulation of MCP-1 and CD68 mRNA and protein expression in epididymal WAT after L-NAME treatment, especially in HFD-fed mice. MCP-1, a potent chemotactic factor that induces monocyte recruitment (16) and inflammatory response (31), has recently been recognized as a key adipokine to induce adipose inflammation and insulin resistance in the obese state (14); MCP-1 abundantly expressed in WAT increases in plasma in obese mice, whereas MCP-1-null mice

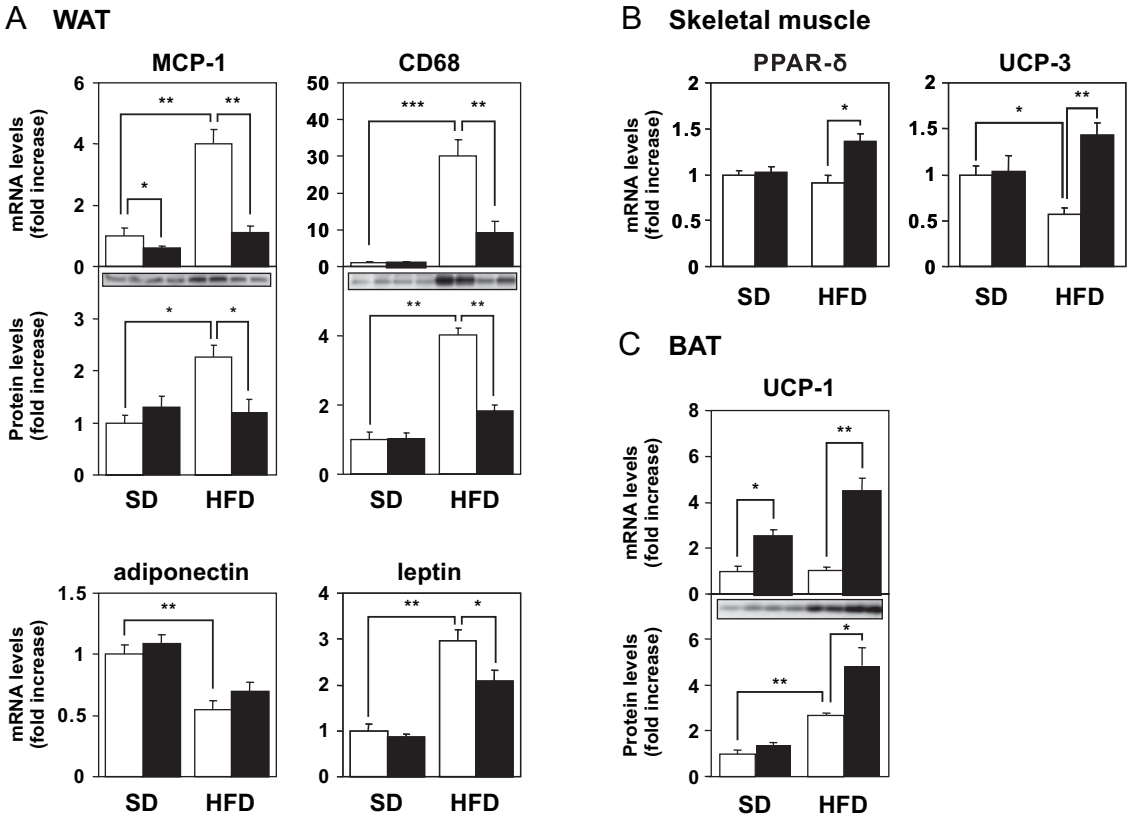

FIG. 5. Changes in a set of gene and protein expression in adipose tissue and skeletal muscle. The steady-state mRNA and/or protein levels for MCP-1 and CD68 and mRNA levels for adiponectin and leptin in epididymal WAT (A), PPAR-δ and UCP-3 in soleus muscle (B), and UCP-1 in interscapular BAT (C) from SD- and HFD-fed mice treated with (*black column*) or without (*white column*) L-NAME are shown. Each *column* is the mean of four to six independent animals expressed as fold increase over control SD-fed mice treated without L-NAME. *, $P < 0.05$, **, $P < 0.01$, and ***, $P < 0.001$ between the indicated groups.

show a marked improvement in obesity-induced insulin resistance and reduced adipose macrophage accumulation. Therefore, a marked reduction of adipose mass in the L-NAME-treated mice and subsequent decrease in MCP-1 and CD68 expression are responsible for reduced adipose inflammation and improved insulin resistance.

The present study also shows that L-NAME treatment up-regulates PPAR-δ mRNA levels in skeletal muscles in HFD-fed mice. PPAR-δ is a member of the nuclear receptor superfamily that enhances fatty acid catabolism and energy uncoupling (18). Treatment with a PPAR-δ agonist causes weight loss and improves insulin resistance by increasing lipid catabolism and oxidative phosphorylation in adipose tissue and skeletal muscle (32). It is noteworthy that the promoter region of mouse PPAR-δ gene contains an activator protein (AP)-1 binding site (33), and NO donor inhibits AP-1 binding activity in murine endothelial cell (34). Thus, it is assumed that NO blockade by L-NAME may increase AP-1-mediated transactivation of PPAR-δ gene, thereby contributing partly to decreased adiposity and improved glucose intolerance in HFD-induced obese mice.

Our data also show that UCP-3, a member of the mitochondrial transporter superfamily involved in regulation of fatty acid oxidation (17), is up-regulated in skeletal muscle after L-NAME treatment. Mice with muscle-specific UCP-3 overexpression display reduced adiposity, improved glucose tolerance, and high energy expenditure (35), whereas mice overexpressing PPAR-δ show improved metabolic phenotypes with concomitant increase in UCP-3 expression in skeletal muscle (32). Furthermore, UCP-3 expression is mainly enhanced by PPAR-δ activation in L6 myocytes (36). Taken together, the enhanced UCP-3 expression via PPAR-δ activation in skeletal muscle could also reduce adiposity and improve glucose intolerance.

In the present study, both eNOS constitutively expressed in WAT, BAT, and skeletal muscle remain unchanged after HFD feeding, but iNOS in WAT and skeletal muscle markedly increases after HFD feeding, suggesting that increased NO production caused by HFD feeding in WAT and skeletal muscle is mainly derived from iNOS. Furthermore, the present study showed that HFD-induced up-regulation of iNOS mRNA in skeletal muscle is markedly decreased after L-NAME treatment. Our data are consistent with those of previous studies demonstrating an inhibitory effect of L-NAME on iNOS mRNA overexpression (37, 38). In addition, mice disrupted with eNOS and/or nNOS gene exhibit insulin resistance (8, 39), whereas iNOS-null mice averts obesity-linked insulin resistance (7). Thus, NO possesses bidirectional, beneficial, and detrimental actions on glucose homeostasis; physiological amounts of NO produced by either eNOS or nNOS play a protective role in the regulation of glucose homeostasis, whereas iNOS-mediated overpro-

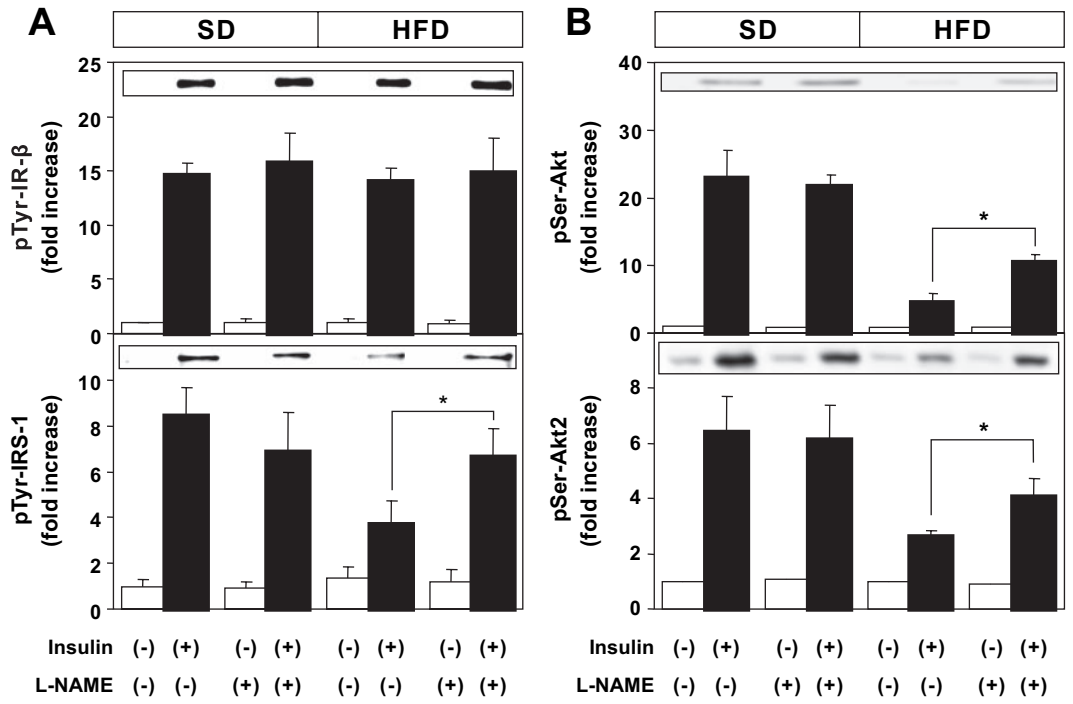

FIG. 6. Changes of insulin signaling in skeletal muscle. Immunoblottings of insulin-stimulated tyrosine phosphorylation of IR-β (*upper panel*) and IRS-1 (*lower panel*) (A) and serine phosphorylation of Akt (*upper panel*) and Akt2 (*lower panel*) (B) in soleus muscle from SD- and HFD-fed mice treated with or without L-NAME are shown. Each *column* is the mean from four independent animals, expressed as fold increase over control SD-fed mice without insulin stimulation. *, $P < 0.05$ between the indicated groups.

duction of NO leads to insulin resistance. The present experimental model of total NOS blockade showed metabolic phenotypes very similar to iNOS-null mice, suggesting that excess NO production derived from iNOS induction after a HFD could play a pivotal role in the development of obesity-induced insulin resistance.

It should be noted that insulin-stimulated tyrosine phosphorylation of IRS-1 and serine phosphorylation of Akt, including Akt2 isotype, are preserved in skeletal muscle of L-NAME-treated obese mice. There are three Akt isoforms (1–3) with distinct but overlapping signaling roles (40). Akt-2-null mice displayed impaired glucose tolerance and reduced insulin-stimulated glucose uptake (41), whereas Akt1-null mice have normal glucose homeostasis (42), suggesting that Akt2 is a more relevant isoform for mediating the effect of insulin on glucose transport. Therefore, our results with preserved serine phosphorylation of Akt2 as well as total Akt in skeletal muscle from L-NAME-treated obese mice suggest that enhanced insulin signaling could partly contribute to the improvement of glucose intolerance.

In summary, chronic NO blockade by L-NAME ameliorated HFD-induced adiposity, accompanied by reduced adipose inflammation and improved insulin signaling in skeletal muscle. The reduced adiposity was not due to altered eating behavior but possibly due to increased energy expenditure. Chronic NO inhibition was concomitantly associated with modulation of genes related to inflammation, glucose and lipid metabolism, and thermogenesis. Thus, it is suggested that endogenous NO plays a modulatory role in the development of obesity-induced insulin resistance.

Acknowledgments

Received October 6, 2006. Accepted June 13, 2007.

Address all correspondence and requests for reprints to: Yukio Hirata, M.D., Ph.D., Department of Clinical and Molecular Endocrinology, Tokyo Medical and Dental University Graduate School, 1-5-45 Yushima, Bunkyo-ku, Tokyo 113-8519, Japan. E-mail: ktsuchiya.cme@tmd.ac.jp.

This work was supported in part by Grants-in-Aids from the Ministry of Education, Science, Sports, Culture, and Technology and the Ministry of Health, Labor, and Welfare, of Japan.

Disclosure Statement: The authors have nothing to disclose.

References

1. **Moncada S, Palmer RM, Higgs EA** 1991 Nitric oxide: physiology, pathophysiology, and pharmacology. Pharmacol Rev 43:109–142
2. **Ribiere C, Jaubert AM, Gaudiot N, Sabourault D, Marcus ML, Boucher JL, Denis-Henriot D, Giudicelli Y** 1996 White adipose tissue nitric oxide synthase: a potential source for NO production. Biochem Biophys Res Commun 222:706–712
3. **Andersson K, Gaudiot N, Ribiere C, Elizalde M, Giudicelli Y, Arner P** 1999 A nitric oxide-mediated mechanism regulates lipolysis in human adipose tissue *in vivo*. Br J Pharmacol 126:1639–1645
4. **Kapur S, Bedard S, Marcotte B, Cote CH, Marette A** 1997 Expression of nitric oxide synthase in skeletal muscle: a novel role for nitric oxide as a modulator of insulin action. Diabetes 46:1691–1700
5. **Higaki Y, Hirshman MF, Fujii N, Goodyear LJ** 2001 Nitric oxide increases glucose uptake through a mechanism that is distinct from the insulin and contraction pathways in rat skeletal muscle. Diabetes 50:241–247
6. **Nathan C** 1997 Inducible nitric oxide synthase: what difference does it make? J Clin Invest 100:2417–2423
7. **Perreault M, Marette A** 2001 Targeted disruption of inducible nitric oxide synthase protects against obesity-linked insulin resistance in muscle. Nat Med 7:1138–1143
8. **Cook S, Hugli O, Egli M, Menard B, Thalmann S, Sartori C, Perrin C, Nicod P, Thorens B, Vollenweider P, Scherrer U, Burcelin R** 2004 Partial gene deletion of endothelial nitric oxide synthase predisposes to exaggerated high-fat diet-induced insulin resistance and arterial hypertension. Diabetes 53:2067–2072

9. **Fujimoto M, Shimizu N, Kunii K, Martyn JA, Ueki K, Kaneki M** 2005 A role for iNOS in fasting hyperglycemia and impaired insulin signaling in the liver of obese diabetic mice. Diabetes 54:1340–1348
10. **Morley JE, Kumar VB, Mattammal M, Villareal DT** 1995 Measurement of nitric oxide synthase and its mRNA in genetically obese (ob/ob) mice. Life Sci 57:1327–1331
11. **Morley JE, Flood JF** 1994 Effect of competitive antagonism of NO synthetase on weight and food intake in obese and diabetic mice. Am J Physiol 266: R164–R168
12. **Morley JE, Flood JF** 1992 Competitive antagonism of nitric oxide synthetase causes weight loss in mice. Life Sci 51:1285–1289
13. **Morley JE, Flood JF** 1991 Evidence that nitric oxide modulates food intake in mice. Life Sci 49:707–711
14. **Kanda H, Tateya S, Tamori Y, Kotani K, Hiasa K, Kitazawa R, Kitazawa S, Miyachi H, Maeda S, Egashira K, Kasuga M** 2006 MCP-1 contributes to macrophage infiltration into adipose tissue, insulin resistance, and hepatic steatosis in obesity. J Clin Invest 116:1494–1505
15. **Neels JG, Olefsky JM** 2006 Inflamed fat: what starts the fire? J Clin Invest 116:33–35
16. **Matsushima K, Larsen CG, DuBois GC, Oppenheim JJ** 1989 Purification and characterization of a novel monocyte chemotactic and activating factor produced by a human myelomonocytic cell line. J Exp Med 169:1485–1490
17. **Brand MD, Esteves TC** 2005 Physiological functions of the mitochondrial uncoupling proteins UCP2 and UCP3. Cell Metab 2:85–93
18. **Barish GD, Narkar VA, Evans RM** 2006 PPARΔ: a dagger in the heart of the metabolic syndrome. J Clin Invest 116:590–597
19. **Koyanagi M, Egashira K, Kitamoto S, Ni W, Shimokawa H, Takeya M, Yoshimura T, Takeshita A** 2000 Role of monocyte chemoattractant protein-1 in cardiovascular remodeling induced by chronic blockade of nitric oxide synthesis. Circulation 102:2243–2248
20. **Katsuyama K, Shichiri M, Kato H, Imai T, Marumo F, Hirata Y** 1999 Differential inhibitory actions by glucocorticoid and aspirin on cytokine-induced nitric oxide production in vascular smooth muscle cells. Endocrinology 140: 2183–2190
21. **Saller CF, Salama AI** 1984 Rapid automated analysis of biogenic amines and their metabolites using reversed-phase high-performance liquid chromatography with electrochemical detection. J Chromatogr 309:287–298
22. **Yoshimoto T, Fukai N, Sato R, Sugiyama T, Ozawa N, Shichiri M, Hirata Y** 2004 Antioxidant effect of adrenomedullin on angiotensin II-induced reactive oxygen species generation in vascular smooth muscle cells. Endocrinology 145:3331–3337
23. **Chander V, Chopra K** 2006 Possible role of nitric oxide in the protective effect of resveratrol in 5/6th nephrectomized rats. J Surg Res 133:129–135
24. **Fang TC, Wu CC, Huang WC** 2001 Inhibition of nitric oxide synthesis accentuates blood pressure elevation in hyperinsulinemic rats. J Hypertens 19:1255–1262
25. **Kvetnansky R, Pacak K, Tokarev D, Jelokova J, Jezova D, Rusnak M** 1997 Chronic blockade of nitric oxide synthesis elevates plasma levels of catecholamines and their metabolites at rest and during stress in rats. Neurochem Res 22:995–1001
26. **Navarro J, Sanchez A, Saiz J, Ruilope LM, Garcia-Estan J, Romero JC, Moncada S, Lahera V** 1994 Hormonal, renal, and metabolic alterations during hypertension induced by chronic inhibition of NO in rats. Am J Physiol 267: R1516–R1521
27. **Egi Y, Matsumura Y, Murata S, Umekawa T, Hisaki K, Takaoka M, Morimoto S** 1994 The effects of NG-nitro-L-arginine, a nitric oxide synthase inhibitor, on norepinephrine overflow and antidiuresis induced by stimulation of renal nerves in anesthetized dogs. J Pharmacol Exp Ther 269:529–535
28. **Lafontan M, Berlan M** 1993 Fat cell adrenergic receptors and the control of white and brown fat cell function. J Lipid Res 34:1057–1091
29. **Nicholls PJ, Malcolm AD** 1989 Nucleic acid analysis by sandwich hybridization. J Clin Lab Anal 3:122–135
30. **Lowell BB, Spiegelman BM** 2000 Towards a molecular understanding of adaptive thermogenesis. Nature 404:652–660
31. **Viedt C, Vogel J, Athanasiou T, Shen W, Orth SR, Kubler W, Kreuzer J** 2002 Monocyte chemoattractant protein-1 induces proliferation and interleukin-6 production in human smooth muscle cells by differential activation of nuclear factor-κB and activator protein-1. Arterioscler Thromb Vasc Biol 22:914–920
32. **Wang YX, Zhang CL, Yu RT, Cho HK, Nelson MC, Bayuga-Ocampo CR, Ham J, Kang H, Evans RM** 2004 Regulation of muscle fiber type and running endurance by PPARΔ. PLoS Biol 2:e294
33. **Tan NS, Michalik L, Noy N, Yasmin R, Pacot C, Heim M, Fluhmann B, Desvergne B, Wahli W** 2001 Critical roles of PPARβ/Δ in keratinocyte response to inflammation. Genes Dev 15:3263–3277
34. **Berendji-Grun D, Kolb-Bachofen V, Kroncke KD** 2001 Nitric oxide inhibits endothelial IL-1[β]-induced ICAM-1 gene expression at the transcriptional level decreasing Sp1 and AP-1 activity. Mol Med 7:748–754
35. **Clapham JC, Arch JR, Chapman H, Haynes A, Lister C, Moore GB, Piercy V, Carter SA, Lehner I, Smith SA, Beeley LJ, Godden RJ, Herrity N, Skehel M, Changani KK, Hockings PD, Reid DG, Squires SM, Hatcher J, Trail B, Latcham J, Rastan S, Harper AJ, Cadenas S, Buckingham JA, Brand MD, Abuin A** 2000 Mice overexpressing human uncoupling protein-3 in skeletal muscle are hyperphagic and lean. Nature 406:415–418
36. **Solanes G, Pedraza N, Iglesias R, Giralt M, Villarroya F** 2003 Functional relationship between MyoD and peroxisome proliferator-activated receptor-dependent regulatory pathways in the control of the human uncoupling protein-3 gene transcription. Mol Endocrinol 17:1944–1958
37. **Cui L, Takagi Y, Wasa M, Sando K, Khan J, Okada A** 1999 Nitric oxide synthase inhibitor attenuates intestinal damage induced by zinc deficiency in rats. J Nutr 129:792–798
38. **Hsieh JS, Wang JY, Lin SR, Lian ST, Chen FM, Hsieh MC, Huang TJ** 2003 Overexpression of inducible nitric oxide synthase in gastric mucosa of rats with portal hypertension: correlation with gastric mucosal damage. J Surg Res 115:24–32
39. **Shankar RR, Wu Y, Shen HQ, Zhu JS, Baron AD** 2000 Mice with gene disruption of both endothelial and neuronal nitric oxide synthase exhibit insulin resistance. Diabetes 49:684–687
40. **Walker KS, Deak M, Paterson A, Hudson K, Cohen P, Alessi DR** 1998 Activation of protein kinase Bβ and γ isoforms by insulin *in vivo* and by 3-phosphoinositide-dependent protein kinase-1 *in vitro*: comparison with protein kinase Bα. Biochem J 331:299–308
41. **Cho H, Mu J, Kim JK, Thorvaldsen JL, Chu Q, Crenshaw 3rd EB, Kaestner KH, Bartolomei MS, Shulman GI, Birnbaum MJ** 2001 Insulin resistance and a diabetes mellitus-like syndrome in mice lacking the protein kinase Akt2 (PKBβ). Science 292:1728–1731
42. **Cho H, Thorvaldsen JL, Chu Q, Feng F, Birnbaum MJ** 2001 Akt1/PKBα is required for normal growth but dispensable for maintenance of glucose homeostasis in mice. J Biol Chem 276:38349–38352

***Endocrinology* is published monthly by The Endocrine Society (http://www.endo-society.org), the foremost professional society serving the endocrine community.**